

Article

Influence of Meteorological Factors and Chemical Processes on the Explosive Growth of PM_{2.5} in Shanghai, China

Wenwen Sun ^{1,2}, Juntao Huo ³, Qingyan Fu ³, Yuxin Zhang ² and Xiangde Lin ^{4,*}

¹ Department of Research, Shanghai University of Medicine & Health Sciences Affiliated Zhoupu Hospital, Shanghai 201318, China; sunww@sumhs.edu.cn

² College of Medical Technology, Shanghai University of Medicine & Health Sciences, Shanghai 201318, China; zyx032901@163.com

³ Shanghai Environmental Monitoring Center, Shanghai 200235, China; huojt@sheemc.cn (J.H.); qingyanf@sheemc.cn (Q.F.)

⁴ School of Medical Instrument, Shanghai University of Medicine & Health Sciences, Shanghai 201318, China

* Correspondence: linxd@sumhs.edu.cn; Tel.: +86-156-2151-2252

Abstract: In order to explore the mechanism of haze formation, the meteorological effect and chemical reaction process of the explosive growth (EG) of PM_{2.5} were studied. In this study, the level of PM_{2.5}, water-soluble inorganic ions, carbonaceous aerosols, gaseous precursors, and meteorological factors were analyzed in Shanghai in 2018. The EG event is defined by a net increase of PM_{2.5} mass concentration greater than or equal to 100 µg m⁻³ within 3, 6, or 9 h. The results showed that the annual average PM_{2.5} concentration in Shanghai in 2018 was 43.2 µg m⁻³, and secondary inorganic aerosols and organic matter (OM) accounted for 55.8% and 20.1% of PM_{2.5}, respectively. The increase and decrease in the contributions of sulfate, nitrate, ammonium (SNA), and elemental carbon (EC) to PM_{2.5} from clean days to EG, respectively, indicated a strong, secondary transformation during EG. Three EG episodes (Ep) were studied in detail, and the PM_{2.5} concentration in Ep3 was highest (135.7 µg m⁻³), followed by Ep2 (129.6 µg m⁻³), and Ep1 (82.3 µg m⁻³). The EG was driven by stagnant conditions and chemical reactions (heterogeneous and gas-phase oxidation reactions). This study improves our understanding of the mechanism of haze pollution and provides a scientific basis for air pollution control in Shanghai.

Keywords: fine particle; explosive growth; mechanism; meteorological factors; chemical reaction process



Citation: Sun, W.; Huo, J.; Fu, Q.; Zhang, Y.; Lin, X. Influence of Meteorological Factors and Chemical Processes on the Explosive Growth of PM_{2.5} in Shanghai, China. *Atmosphere* **2022**, *13*, 1068. <https://doi.org/10.3390/atmos13071068>

Academic Editor: Roberto Bellasio

Received: 16 June 2022

Accepted: 4 July 2022

Published: 6 July 2022

Publisher's Note: MDPI stays neutral with regard to jurisdictional claims in published maps and institutional affiliations.



Copyright: © 2022 by the authors. Licensee MDPI, Basel, Switzerland. This article is an open access article distributed under the terms and conditions of the Creative Commons Attribution (CC BY) license (<https://creativecommons.org/licenses/by/4.0/>).

1. Introduction

Since persistent haze pollution was experienced in Eastern China in January 2013, fine particulate matter of less than 2.5 µm in diameter (PM_{2.5}) has attracted widespread, national attention as a key component of pollution events [1]. The hazy episodes caused severe aerosol pollution events, led to a significant reduction in visibility, affected traffic, constrained local economic development, and greatly damaged the respiratory and circulatory systems of residents [2]. Furthermore, when PM_{2.5} contains hydrophilic components, such as sulfate and nitrate, it can also serve as cloud condensation nuclei (CCN), changing the physical and chemical characteristics of clouds, and thus influencing precipitation as well as the regional climate [3]. Understanding the mechanism of heavy haze is vital to evaluating the influences of PM_{2.5} in regional air quality, regional climate forcing, and human health.

In recent years, many studies have been conducted to investigate the formation mechanisms of heavy haze. PM_{2.5} concentration in the atmosphere is influenced by a variety of factors, such as pollutant emissions, regional transportation, aerosol physicochemical processes, gas–particle conversion, and meteorological conditions [4–7]. Ye et al. [8] concluded that there was a significant relationship between daily PM_{2.5} concentration and meteorological factors, including temperature (T), relative humidity (RH), wind speed (WS), and

wind direction (WD), and they suggested that an increase in RH could promote the growth of $PM_{2.5}$. Meanwhile, $PM_{2.5}$ was negatively correlated with WS; that is, with increases in WS, $PM_{2.5}$ showed a decreasing trend, which was attributed to a high WS helping to disperse $PM_{2.5}$ [8]. Using a stacked system model for the prediction and analysis of daily average $PM_{2.5}$ concentrations in Beijing, Zhai and Chen [9] also learned that local extreme and maximum WS were considered to be the main influences of meteorological factors in the interregional transport of pollutants. The adverse meteorological factors could cause atmospheric advection, atmospheric dispersion, and secondary aerosol formation [10]. Zhong et al. [1] suggested that the cumulative explosive growth (EG) in $PM_{2.5}$ mass in Beijing was mainly influenced by the stable atmospheric stratification characteristics of a southerly breeze or flat wind, anomalous near-surface inversion temperatures, and water vapor accumulation. A study on emission-control downwind of Nanjing during the 2014 Summer Youth Olympic Games suggested that stagnant meteorological conditions and a high RH had a significant effect on the production and accumulation of $PM_{2.5}$, indicating that the seasonal meteorological characteristics were significant for the production of $PM_{2.5}$ [11].

A recent study found that severe haze pollution is largely driven by the formation of secondary aerosols. The formation of the secondary aerosols of sulfate and nitrate were dominated by gas-phase oxidation and heterogeneous reactions, which were enhanced by a high RH [12,13]. Through the research group's repeated, simultaneous observations of the gas-liquid and gas-particle phases of atmospheric peroxides in the Beijing area, Xuan et al. [14] concluded that strong atmospheric oxidation was considered to be a key factor in the rapid increase of secondary, fine particulate matter concentrations during periods of heavy pollution, which was one of the causes of heavy atmospheric pollution in Beijing-Tianjin-Hebei and the surrounding areas in autumn and winter. The formation mechanism of $PM_{2.5}$ is complicated; more field measurements of chemical $PM_{2.5}$ components in different environments are urgently needed.

Therefore, it is meaningful to explore the driving factors of EG to provide useful information to the government, which will enable forecasting and the reduction of severe air pollution. In this study, the meteorological effect and chemical process of EG were explored by analyzing $PM_{2.5}$, water-soluble inorganic ions, carbonaceous substances, gaseous precursors, and meteorological factors in Shanghai in 2018 so as to explore the factors that lead to EG.

2. Materials and Methods

2.1. Sample Site

The observation site was located at 45 km westward from the center of Shanghai in the suburban Qingpu Environmental Monitoring Center (Dianshan Lake Superstation, 31.09° N, 120.98° E). The Qingpu District is bounded by Zhejiang Province to the south and Jiangsu Province to the west. The land use near the observation site included residential areas, agriculture, industry, and highways. Shanghai has a predominantly subtropical monsoon climate with moderate humidity and an annual average temperature of 17.6 °C; it had an RH of 76.5%, a WS of 2.1 m s⁻¹, and a total annual rainfall of 1172.8 mm in 2018. Shanghai is mainly influenced by parts of the Yangtze River Delta (YRD) and North China Plain (NCP) areas in winter; the WD is generally from the northwest and the north. In contrast, Shanghai becomes the contributor of pollutant sources in the summer in the YRD region [15]. The total area of Dianshan Lake reaches 62 km², and it is located 0.2 km to the west and north of the measurement site, resulting in the higher RH of the site.

2.2. Measurement Methods

The $PM_{2.5}$ concentration was measured automatically by a tapered element oscillating microbalance (TEOM 1405-D, Thermo Scientific Co., Waltham, MA, USA). The TEOM flow rate was 16.7 L min⁻¹. The average sampling time was 5 min, which was converted to hourly means. The uncertainty of the hourly measurements was $\pm 1.50 \mu\text{g m}^{-3}$, and the

detection limit was $0.06 \mu\text{g m}^{-3}$. Detailed information about the measurement methods of the instrument can be found in a previously published study [16].

Gas species were measured online by a series of gas analyzers, including an O_3 analyzer (model 49I), a NO/NO_2 analyzer (model 42I), a SO_2 analyzer (model 43I), and a CO analyzer (model 48I; Thermo Scientific, Waltham, MA, USA). The ambient air was connected to the gas analyzer located 1.5 m above the roof with a Teflon tube. The collected gas data were resolved to 1 min and then converted to hourly averages. The TSO_2 , NO_x , and CO gas analyzers were calibrated daily using standard gases of 50 ppmv SO_2 , 52 ppmv NO , and 5000 ppmv CO , with multipoint calibrations performed every 3–6 months. An O_3 analyzer was calibrated by a specific O_3 calibrator (49C PS) and zeroed every 2 h using an internal catalytic converter. The accuracy of the gas analyzers for O_3 , NO/NO_2 , SO_2 , and CO were 1.0, 0.4, 1.0, and 0.1 ppb, respectively. The meteorological parameters, including RH, T, WS, WD, atmospheric pressure (P), precipitation, and visibility, were monitored by an automatic meteorological station which was installed 18 m above the ground on the roof of a building located inside the Qingpu Environmental Monitoring Center. The station registered one datapoint every minute and then converted those into hourly averages.

The MARGA instrument (ADI 2080, Applikon Analytical, Schiedam, The Netherlands) equipped with a $\text{PM}_{2.5}$ cutting head was used to measure water-soluble, inorganic ions at a flow rate of 16.7 L min^{-1} and at a resolution of 1 h. To ensure the accuracy of the data, the MARGA was calibrated using the internal standard method (with bromide as the anion and lithium as the cation) and the external standard method (with a mixture of anions and cations), and the soluble ions in the target water were determined before and after the experiment using the multipoint method. The limits of the detection of NO_3^- , SO_4^{2-} , Cl^- , NH_4^+ , K^+ , Na^+ , Mg^{2+} , and Ca^{2+} were 0.04, 0.01, 0.05, 0.09, 0.05, 0.06, and $0.1 \mu\text{g m}^{-3}$ (based on a sampling time of 45 min), respectively.

Organic carbon (OC) and elemental carbon (EC) concentrations were determined by using an online Sunset semi-continuous carbon analyzer (Sunset Laboratory, Forest Grove, OR, USA) using the thermal–optical transmittance method at a flow rate of 8 L min^{-1} through the $\text{PM}_{2.5}$ cutting head. OC and EC concentrations were collected every 30 min and averaged as hourly data. The accuracy and detection limits were measured by the changes in EC and OC concentrations on exposed filters and blank membranes, respectively. The measurement results were well-correlated with the membrane analysis, with relative standard deviations below 5%. The EC level on the blank membrane was found to be negligible, but the OC concentrations ranged from 0.1 to $1.0 \mu\text{g m}^{-3}$. The detection limits for the OC and EC concentrations were 0.2 and $0.04 \mu\text{g m}^{-3}$, respectively (based on 45 min sampling time).

2.3. Definition of Explosive Growth of $\text{PM}_{2.5}$

EG has been defined in previous studies and is briefly described in this section. Wang et al. [17] defined an increase in $\text{PM}_{2.5}$ concentration in the Beijing–Tianjin–Hebei region from a low concentration ($<35 \mu\text{g m}^{-3}$) to an extremely high concentration ($>500 \mu\text{g m}^{-3}$) within 8 h as an EG event. After this study, Zhong et al. [1] defined an explosive growth event as occurring when a minimum $\text{PM}_{2.5}$ concentration doubles within a few hours (up to 10 h) in Beijing during a period of heavy haze ($\text{PM}_{2.5}$ concentration $> 80 \mu\text{g m}^{-3}$ for 3 consecutive days with a maximum value of $400 \mu\text{g m}^{-3}$ or more). However, most studies on EG have focused on the Beijing area [1,17]. Therefore, given the typical air pollution characteristics of Shanghai, we proposed a definition of EG events that occur within 3, 6, or 9 h, respectively [12]. EG was defined as

$$\text{EG in 3 h : } \Delta\text{PM}_{2.5} \geq 100 \mu\text{g m}^{-3} \text{ and } 0 < \Delta t \leq 3$$

$$\text{EG in 6 h : } \Delta\text{PM}_{2.5} \geq 100 \mu\text{g m}^{-3} \text{ and } 3 < \Delta t \leq 6$$

$$\text{EG in 9 h : } \Delta\text{PM}_{2.5} \geq 100 \mu\text{g m}^{-3} \text{ and } 6 < \Delta t \leq 9$$

3. Results and Discussion

3.1. PM_{2.5} Level

The annual average PM_{2.5} concentration in Shanghai in 2018 was 43.2 µg m⁻³, which was 1.2 times higher than the value recommended by the World Health Organization (WHO; 35 µg m⁻³). This concentration was lower than that of Beijing (135 ± 63 µg m⁻³) [18], but higher than that of Guangdong in 2017 (37.5 µg m⁻³) [19]. Secondary inorganic aerosols accounted for 55.8% of the total PM_{2.5} mass concentration, in which NO₃⁻, SO₄²⁻, and NH₄⁺ accounted for 24.7%, 17.6%, and 13.5%, respectively. The primary ions (Cl⁻, K⁺, Na⁺, Ca²⁺, and Mg²⁺) accounted for only 3.4% of PM_{2.5}. The contribution of OM (OC * 1.8) [20,21] to PM_{2.5} was 20.1%, but that of EC was only 4.2%. The unknown fraction of PM_{2.5} accounted for 22.4%, which may be related to the uncertainty of the OM and OC conversion factors, other unknown species, and the uncertainty of observations.

Compared to other water-soluble ions, the concentration of NO₃⁻ was the highest in Shanghai in 2018, with an annual mean concentration of 10.7 ± 12.1 µg m⁻³, followed by SO₄²⁻ (7.6 ± 5.4 µg m⁻³), NH₄⁺ (5.8 ± 5.6 µg m⁻³), Cl⁻ (1.0 ± 1.0 µg m⁻³), K⁺ (0.20 ± 0.34 µg m⁻³), Na⁺ (0.14 ± 0.18 µg m⁻³), Ca²⁺ (0.07 ± 0.12 µg m⁻³), and Mg²⁺ (0.02 ± 0.04 µg m⁻³). This concentration differs from that of Beijing, where Zhang et al. [18] found that the largest concentration was SO₄²⁻ (13.6 ± 12.4 µg m⁻³), followed by NO₃⁻ (11.3 ± 10.8 µg m⁻³), NH₄⁺ (6.9 ± 7.1 µg m⁻³), Ca²⁺ (1.6 ± 1.4 µg m⁻³), Cl⁻ (1.4 ± 2.2 µg m⁻³), K⁺ (0.92 ± 0.75 µg m⁻³), Na⁺ (0.46 ± 0.55 µg m⁻³), and Mg²⁺ (0.02 ± 0.04 µg m⁻³). This may have been due to the fact that coal combustion is the main winter heating method in North China, compared with Shanghai, moreover, the distance of Beijing to Inner Mongolia was much near. Thus, the higher SO₄²⁻ and Ca²⁺ in Beijing's atmosphere may be related to coal combustion and dusty weather, respectively [22]. In conclusion, NO₃⁻, SO₄²⁻, and NH₄⁺, as secondary, inorganic ions, were the major components of the total inorganic ions (94.0%), which is consistent with previous studies [23]. The annual average concentrations of OC and EC in Shanghai in 2018 were 5.1 ± 3.2 µg m⁻³ and 1.8 ± 1.4 µg m⁻³, respectively. These concentration values are lower than the national carbonaceous aerosols measured by Zhang et al. (OC 16.1 ± 5.2 µg m⁻³ and EC 3.6 ± 0.93 µg m⁻³), but the carbonaceous aerosol concentrations at urban sites were twice as high (OC 33.1 ± 9.6 µg m⁻³ and EC 11.2 ± 2.0 µg m⁻³) [24].

3.2. Seasonal Distribution Characteristics of PM_{2.5} and Chemical PM_{2.5} Components

Figure 1 shows the seasonal variation of the concentrations of PM_{2.5}, major chemical PM_{2.5} components, and gaseous precursors in Shanghai in 2018. The seasonal variation of pollutants is influenced by the intensity of pollutant emissions from sources, atmospheric processes, and meteorological conditions. Unlike Northern China, there is less indoor coal combustion and wood-burning for winter heating in Shanghai due to the higher average winter temperature (5.6 °C). Therefore, the influence of atmospheric processes and meteorological conditions on the seasonal variation of PM_{2.5} is of great important in Shanghai. The highest PM_{2.5} mass concentration was observed in winter (56.5 ± 44.6 µg m⁻³), which was 1.1–1.9 times higher than that of other seasons, followed by spring (50.0 ± 28.7 µg m⁻³), autumn (37.1 ± 16.2 µg m⁻³), and summer (29.4 ± 20.9 µg m⁻³). Stagnant weather conditions, due to frequently calm winds and lower mixed boundary-layer heights, were the main reasons for the highest PM_{2.5} concentrations in winter [25]. However, the lowest PM_{2.5} concentration in summer was attributed to the fact that the rainfall (a total precipitation of 533.5 mm in summer) was mainly concentrated in this period.

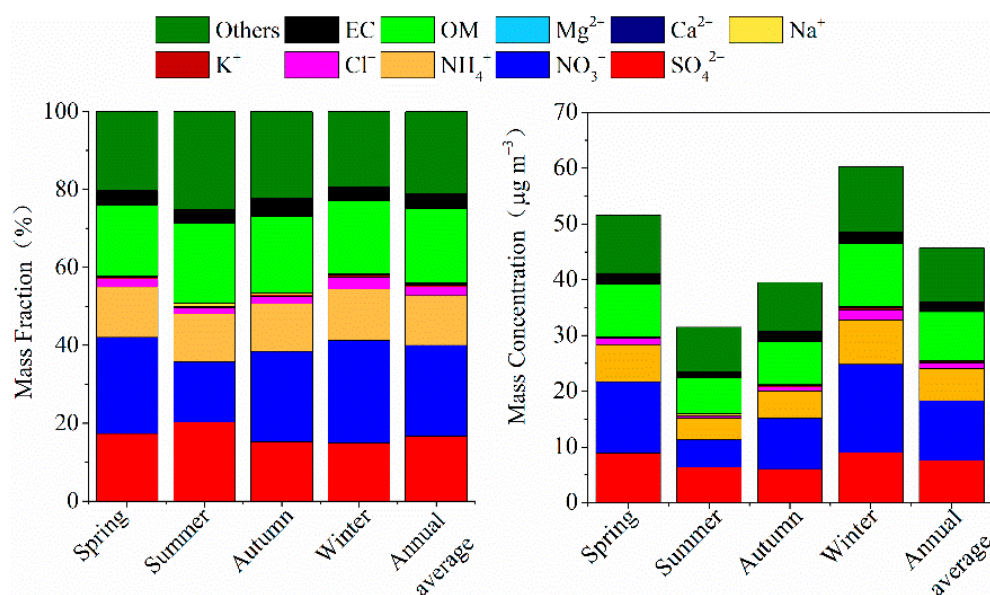


Figure 1. Concentrations and contributions of the chemical PM_{2.5} components for each season.

The seasonal distributions of all major chemical components of PM_{2.5}, except Na⁺, were similar to PM_{2.5}, with highest occurring in winter (Figure 2). The concentration of Na⁺ was highest in summer ($0.23 \pm 0.26 \mu\text{g m}^{-3}$) and lowest in spring ($0.09 \pm 0.14 \mu\text{g m}^{-3}$), and the high level in summer was probably due to the influence of sea-salt aerosols brought by the Shanghai summer monsoon [16]. The seasonal variations of Ca²⁺ and Mg²⁺ were slightly similar, with the highest concentrations registered in winter ($0.11 \pm 0.15 \mu\text{g m}^{-3}$ and $0.03 \pm 0.06 \mu\text{g m}^{-3}$), followed by spring ($0.08 \pm 0.13 \mu\text{g m}^{-3}$ and $0.02 \pm 0.04 \mu\text{g m}^{-3}$). The relatively higher WS and lower RH in spring favored the resuspension of dust, and the more frequent dust storms from northwestern China in spring can transport dust to Shanghai over long distances, causing high Ca²⁺ and Mg²⁺ levels [26]. The concentration of K⁺ showed the highest level in winter ($0.38 \pm 0.57 \mu\text{g m}^{-3}$), followed by autumn ($0.20 \pm 0.04 \mu\text{g m}^{-3}$), measured as being 1.4 and 2.5 times higher in autumn than in spring and summer, respectively, which was closely related with biomass-burning being mainly concentrated in autumn [27]. The level of Cl⁻ exhibited the highest value in winter ($1.8 \pm 1.4 \mu\text{g m}^{-3}$), that being 1.7–3.5 times higher than that in other seasons, which was mainly associated with coal combustion for winter heating and regional transport from Northern China [28].

As shown in Figures 1 and 2, the seasonal contributions of sulfate, nitrate, and ammonium (SNA) to PM_{2.5} varied from 51.3% to 58.0%. Both NO₃⁻ and NH₄⁺ contributed to PM_{2.5} the most in winter and the least in summer, but the seasonal contribution and distribution of SO₄²⁻ was the opposite. The high contribution of SO₄²⁻ in summer was mainly attributed to enhanced photochemical reactions due to the higher temperatures and stronger solar radiation in summer, which is consistent with the findings of Wang et al. [29]. In addition, the higher O₃ concentration ($78.1 \mu\text{g m}^{-3}$) in summer also promoted this seasonal distribution characteristic [30]. Interestingly, the seasonal variation characteristics of SO₄²⁻ and SO₂ were different. SO₂ showed a more pronounced seasonal variation, with the highest value registered in winter, with that being 1.1–1.8 times higher than that in the other seasons, while the SO₄²⁻ level did not exhibit an obvious difference in winter and spring, being 1.4–1.5 times higher than the other seasons. Similarly, the seasonal variation characteristics of NO₃⁻ were more distinct compared with those of NO₂, with the maximum registered in winter ($15.8 \pm 15.6 \mu\text{g m}^{-3}$) and the lowest value registered in summer ($4.9 \pm 6.6 \mu\text{g m}^{-3}$), being 1.2–3.2 times higher in winter than in the other seasons. In contrast, NO₂ exhibited the highest values in autumn ($44.3 \pm 31.1 \mu\text{g m}^{-3}$) and winter ($44.5 \pm 27.1 \mu\text{g m}^{-3}$), with that being 1.2–1.8 times higher than in other seasons.

The levels of SO_4^{2-} and NO_3^- in the atmosphere were influenced by emission sources, such as coal combustion, vehicle emission, and biomass burning; meteorological factors, such as stagnant weather conditions, a high RH, and plenty of sunshine; and complex atmospheric chemical processes, such as heterogeneous reactions, photochemical processes, and gas–particle equilibria. Therefore, the atmospheric chemical processes in Shanghai had a strong influence on the seasonal variation of both SO_4^{2-} and NO_3^- . Previous studies have shown that atmospheric chemical processes led to increases in NO_3^- concentrations in winter at a higher RH and to decreases in NO_3^- concentrations in summer due to the volatilization of ammonium nitrate at a higher temperature [31] and the thermodynamic drive of NH_4NO_3 [32], thus increasing the seasonal distribution gap of NO_3^- between winter and summer.

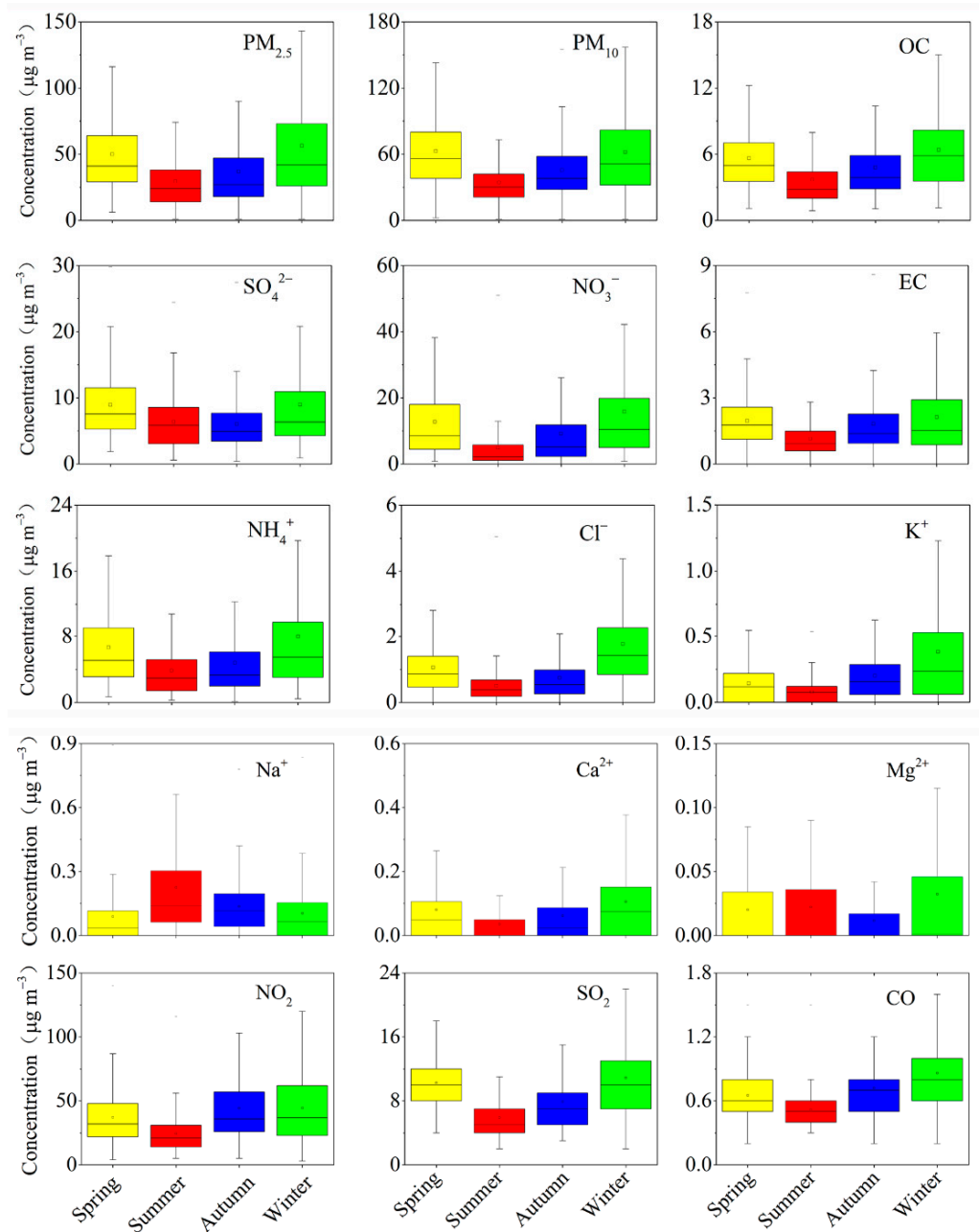


Figure 2. Seasonal distributions of chemical $\text{PM}_{2.5}$ components and gas pollutants. Note that the middle horizontal line, small rectangle, up-line, and the down-line of each histogram denotes the median, average, 25% quantile, and 75% quantile, respectively. The short lines, located above and below each histogram, represent the maximum and minimum values, respectively.

OC and EC had similar seasonal distribution trends, with the highest values in winter ($6.4 \pm 3.6 \mu\text{g m}^{-3}$ and $2.1 \pm 1.8 \mu\text{g m}^{-3}$), being 1.1–1.7 and 1.1–1.9 times higher than those of the other seasons, respectively, and the lowest in summer ($3.7 \pm 2.6 \mu\text{g m}^{-3}$ and $1.1 \pm 0.9 \mu\text{g m}^{-3}$). This distribution characteristic was similar to that found by a previous study performed by Zhang et al. [24], who conducted continuous observations of OC and EC at 18 background and urban sites in China, finding that both were highest in winter and lowest in summer. This seasonal variation may be mainly influenced by emissions intensity and meteorological conditions, for instance, low-molecular semi-volatile organic compounds exist mainly in a gas phase at high temperatures in summer [33]. Studies have shown that secondary organics were present when the ratio of OC/EC was more than 2 [34]. In the present study, the OC/EC ratio averaged 2.8 throughout the year, with ratios of 2.9, 3.1, 2.6, and 2.9 in spring, summer, autumn, and winter, respectively, indicating the existence of secondary organics in Shanghai. Similar to OC, the concentration of secondary organic carbon (SOC) was highest in winter, which was mainly attributed to the enhanced coalescence process of SOC at lower temperatures [35]. In contrast, higher temperatures in summer favored gas–particle separation in the gas phase, therefore limiting the formation of SOC [36]. The contribution of carbonaceous substances to $\text{PM}_{2.5}$ was roughly the same as the seasonal distribution of SNA, accounting for 22.9–25.9% of $\text{PM}_{2.5}$. Although the highest concentrations of OM and EC were in winter, the contribution of OM to $\text{PM}_{2.5}$ was highest in summer (21.8%) and lowest in spring (18.9%), and the contribution of EC was lowest in spring and winter (both 3.9%) and highest in autumn (5.0%), suggesting SNA was the main driving factor for hazy days in winter.

3.3. Chemical Composition Characteristics of Explosive Growth and Clean Days

To deeply study the mechanism of EG in Shanghai, the concentration and contribution of chemical components in $\text{PM}_{2.5}$ during clean days (CDs) and during explosive growth in Shanghai in 2018 were compared (Figure 3). Considering the National Air Quality Standards in China (the second grade of the $\text{PM}_{2.5}$ daily average mass concentrations; $75 \mu\text{g m}^{-3}$) and the $\text{PM}_{2.5}$ concentrations in this work, $\text{PM}_{2.5}$ mass concentrations below $75 \mu\text{g m}^{-3}$ were defined as CDs. A net increase of $\text{PM}_{2.5}$ concentration more than or equal to $100 \mu\text{g m}^{-3}$ within 3, 6, or 9 h was defined as EG.

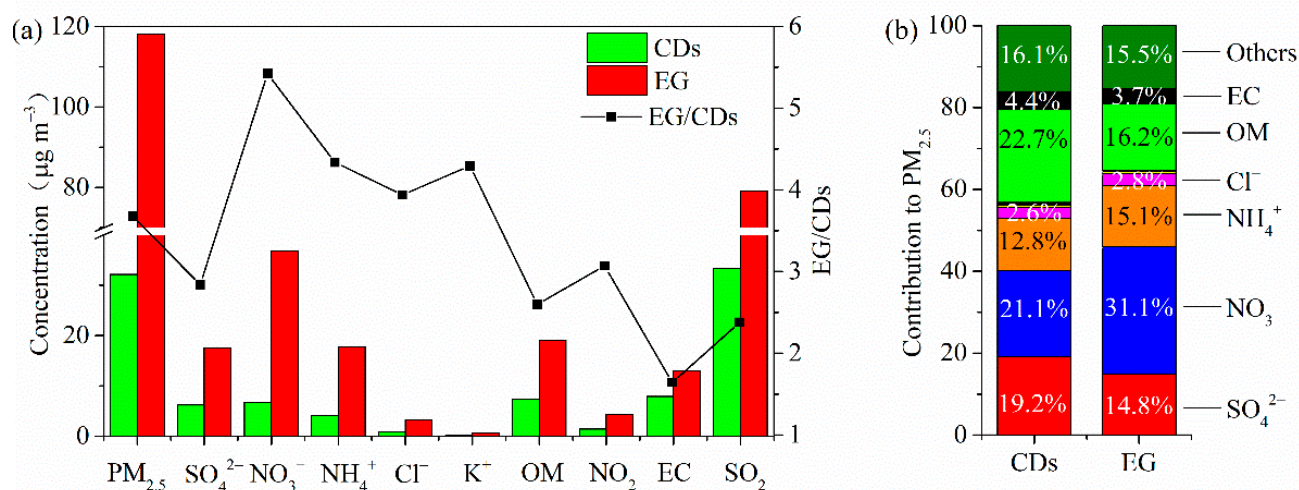


Figure 3. Concentrations of $\text{PM}_{2.5}$, ions, carbonaceous compounds, and gas precursors (a); and contributions of chemical $\text{PM}_{2.5}$ components (b) during CDs and EG.

As shown in Figure 3a, the concentrations of $\text{PM}_{2.5}$, water-soluble ions, carbonaceous substances, and gaseous precursors increased significantly during EG compared to CDs. $\text{PM}_{2.5}$ concentration ($118.1 \mu\text{g m}^{-3}$) was 3.7 times higher in EG periods than on CDs ($32.1 \mu\text{g m}^{-3}$), with SNA being 2.8–5.4 times higher, as well as OM and EC being 2.6–3.1 times higher. The different increase rates of each chemical component of $\text{PM}_{2.5}$

indicated that the contribution to EG of each chemical component was different. The largest growth was NO_3^- (5.4 times higher in EG periods than that of CDs), comparable increases in NH_4^+ , K^+ , and Cl^- (about 4 times higher), and the minimum enhancement was OM (2.6 times), indicating that both primary emissions and secondary transformations contributed to the EG. Both SO_2 and NO_2 increased during EG periods, but a larger growth in NO_2 suggested that nitrogenous substances contributed more to the EG.

As shown in Figure 3b, the contribution of SNA during periods of EG (61%) was greater than that of CDs (53.1%), but the contribution of OM exhibited the opposite distribution. The results were in general agreement with a previous study that found that the contributions of SNA and OM to $\text{PM}_{2.5}$ differed between the eastern coastal region of China and the North China Plain, and the contribution of SNA increased and decreased distinctly on hazy days and clean days, respectively, but it was contrary to OM [37]. Among SNA, NO_3^- contributed the most during EG, rising from 21.1% on CDs to 31.1% during EG. Similarly, NH_4^+ increased from 12.8% on CDs to 15.1% during EG; however, SO_4^{2-} decreased from 19.2% on the CDs to 14.8% during EG. The increase in the percentage of SNA combined with the decrease in EC (from 4.9% on CDs to 3.9% during EG periods) indicated a strong secondary transformation process during EG. Such enhancement of secondary transformations may be related to stagnant weather conditions (e.g., WS less than 1.5 m s^{-1} in this study) and higher gas precursor levels, which accelerated the production and accumulation of secondary aerosols. To some degree, the higher contribution of NO_3^- during EG was also associated with higher RH and lower T in winter, and such meteorological conditions favored the conversion of the gaseous precursor NO_2 to NO_3^- .

3.4. Case Study of Typical Explosive Growth Episodes

A total of 3 explosive growth episodes (Ep) occurred in Shanghai in 2018, 2 in winter and 1 in autumn, with a total duration of 21 h. Ep1 occurred from 08:00 to 13:00 on 15 January 2018; Ep2 occurred from 23:00 on 22 January to 06:00 on 23 January 2018; and Ep3 occurred from 10:00 to 16:00 on 27 November 2018. The highest $\text{PM}_{2.5}$ concentration was measured in Ep3, with $135.7 \mu\text{g m}^{-3}$, followed by Ep2 ($129.6 \mu\text{g m}^{-3}$), and Ep1 ($82.3 \mu\text{g m}^{-3}$). As shown in Figure 4, the contributions of chemical components in Ep2 and Ep3 were relatively similar, with the largest contributions being NO_3^- (39% and 42%, respectively), followed by NH_4^+ (both 19%), and SO_4^{2-} (19% and 18%, respectively). The contributions of OM and EC in Ep1 (29.9% and 8%) were highest, measuring more than twice the amounts registered in other EG events. The contribution of POC was also the highest in Ep1 (9.7%), 1.8 and 2.7 times higher than that in Ep2 (5.5%) and Ep3 (3.6%), respectively; however, the contribution of SOC was the highest in Ep3 (7.0%). The above results suggested that Ep1 was mainly driven by primary pollutants, while secondary aerosols were the main influencing factors in Ep2 and Ep3.

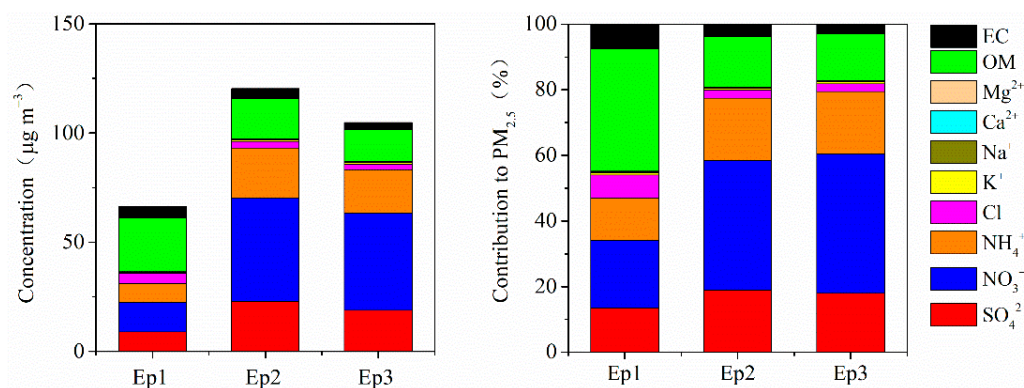


Figure 4. Concentrations and contributions of chemical $\text{PM}_{2.5}$ components during EG.

As shown in Figure 5, the O_3 concentration was lower in Ep2 ($<20 \mu\text{g m}^{-3}$) and higher in Ep1 (a maximum of $70 \mu\text{g m}^{-3}$) and Ep3 (a maximum of $100 \mu\text{g m}^{-3}$). Moreover, Ep2

occurred at night, and Ep1 and Ep3 occurred during the day. Zheng et al. [38] have shown that O_3 is usually used as an indicator of photochemical processes. In addition, there was clearly a daily variation of O_3 in this study, with the highest concentration at noon and lower values in the morning and evening (Figure 5), which was typical of photochemical processes [39]. The results were comparable to the existing conclusions that sunny days could trigger stronger photochemical reactions between 12:00 and 18:00 [40]. Therefore, the photochemical reaction was stronger during Ep1 and Ep3, while it was weaker in Ep2, implying different chemical formation mechanisms for Ep1, Ep3, and Ep2. The strong photochemical activities during Ep1 and Ep3 could generate sufficient oxidants (OH and H_2O_2 radicals) for gas-phase oxidation [41]. As T gradually increased and a strong photochemical effect occurred, it was beneficial to secondary aerosol formation by gas-particle oxidation reactions in Ep1 and Ep3. However, the percentage of secondary inorganic ions was lower in Ep1, along with the lower RH (64.3%) and wind speed (0.8 m s^{-1}) in Ep1 (Figure 6 and Table 1), it was demonstrated that Ep1 was mainly influenced by gas-particle oxidation reactions.

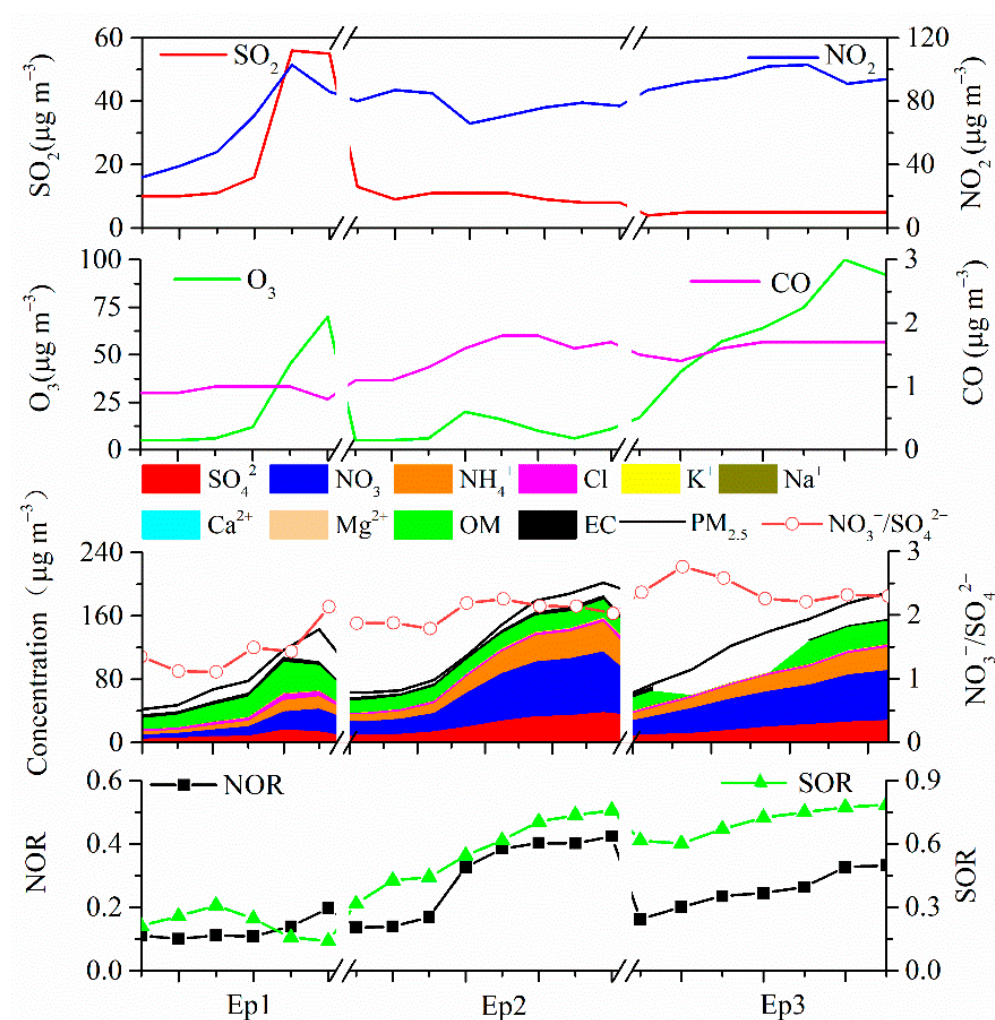


Figure 5. Time trend of $PM_{2.5}$, chemical components, and gas compounds during EG.

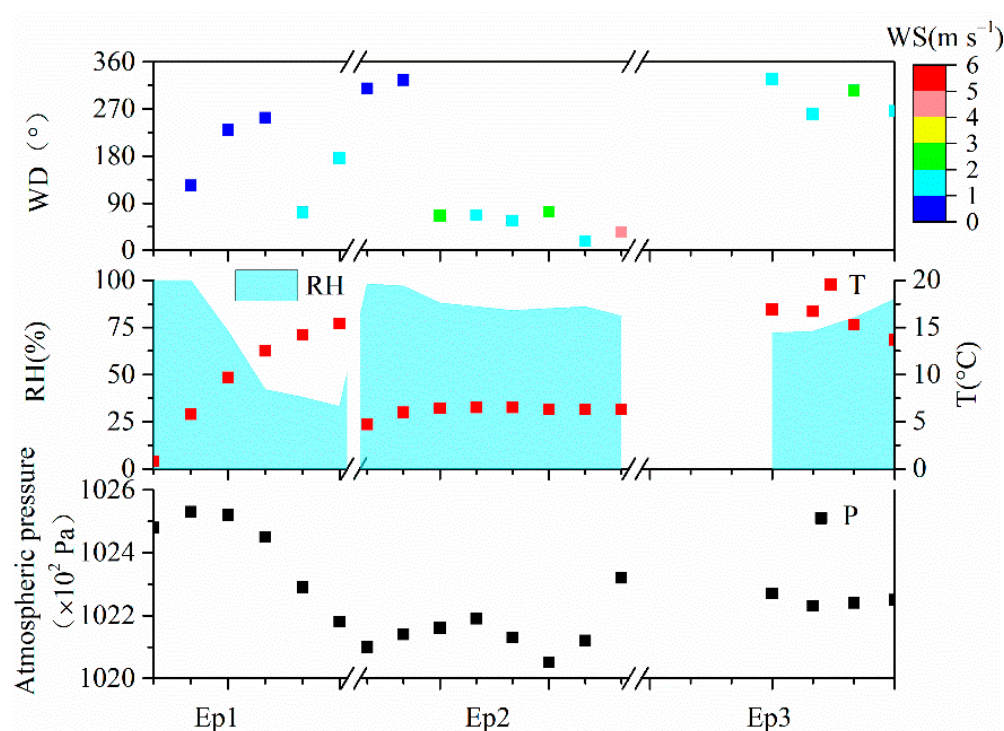


Figure 6. Horizontal ground meteorological conditions during EG.

Table 1. Meteorological factors and PM_{2.5} concentration during CDs and EG.

	T (°C)	RH (%)	WS (m s ⁻¹)	PM _{2.5} (µg m ⁻³)
Ep1	9.7	64.3	0.82	82.3
Ep2	6.1	88.1	1.9	129.6
Ep3	15.7	78.8	1.7	135.7
CDs	18.4	76.7	2.2	32.1

It has been shown that stagnant weather conditions, higher RH, and primary emissions are the important causes in triggering atmospheric particulate-matter pollution [38]. The concentrations of NO₂ gaseous precursors were higher in EG episodes (63.2 µg m⁻³, 77.6 µg m⁻³, and 94.9 µg m⁻³ for Ep1, Ep2, and Ep3, respectively), but SO₂ concentrations were higher only in Ep1 (26.3 µg m⁻³, 10.0 µg m⁻³, and 4.9 µg m⁻³ for Ep1, Ep2, and Ep3, respectively). The concentrations of secondary inorganic ions (NO₃⁻ and SO₄²⁻) were low in Ep1, which was probably due to the low NOR (0.13) and SOR (0.22). Although the concentration of NO₂ was high in Ep2 and Ep3, that of SO₂ was lower than that in Ep1; thus, the high concentrations of the secondary inorganic ions NO₃⁻ and SO₄²⁻ were closely related to the high NOR (0.29 and 0.25 for Ep2 and Ep3, respectively) and SOR (0.57 for Ep2 and 0.7 for Ep3). Apart from the effect of gas precursors, the chemical reaction was also influenced by weather conditions. The obvious enhancement of the RH during hazy days on the North China Plain promoted the liquid-phase formation of secondary inorganic aerosols, leading to a rapid increase in SO₄²⁻ and NO₃⁻ concentrations [38,39]. In this study, the higher RH and proportions of secondary aerosols in Ep2 and Ep3 suggested that the high RH played a crucial role in the formation of explosive growth in Shanghai. The lower planetary boundary-layer (PBL) height, WS, and T during EG tended to form stagnant weather conditions, making it difficult for pollutants to disperse, accompanied by a high RH, which was conducive to the secondary transformation of gaseous pollutants [42,43]. Combining the high RH (88.1%) and lower O₃ (9.9 µg m⁻³) level in Ep2, implies that Ep2 was dominated by heterogeneous reaction. However, both the RH (76.7%) and O₃ (63.7 µg m⁻³) were high in Ep3; therefore, Ep3 was simultaneously influenced by gas-phase oxidation and heterogeneous reactions.

4. Conclusions

To further determine the mechanism of pollution formation, this study deeply explored the chemical reaction process and meteorological effects of EG episodes by analyzing PM_{2.5}, water-soluble inorganic ions, carbonaceous substances, gaseous precursors, and meteorological factors in Shanghai in 2018. The annual average concentration of PM_{2.5} in Shanghai in 2018 was 43.2 $\mu\text{g m}^{-3}$, and NO₃⁻, SO₄²⁻, NH₄⁺, and OM were the main chemical components of PM_{2.5}, accounting for 75.9% of PM_{2.5}. The seasonal variation showed that the highest value of PM_{2.5} in Shanghai in 2018 was in winter (56.5 \pm 44.6 $\mu\text{g m}^{-3}$), which was about 2 times higher than that in summer (29.4 \pm 20.9 $\mu\text{g m}^{-3}$). The difference in seasonal distribution of gas precursors (NO₂ and SO₂) and secondary ions (NO₃⁻ and SO₄²⁻) indicated that atmospheric chemical processes have an important influence on levels of both SO₄²⁻ and NO₃⁻. The increases and decreases in the percentage of SNA and EC from CDs to EG, respectively, indicated a strong secondary transformation during the EG.

The concentration of PM_{2.5} during EG in Shanghai in 2018 was 3.7 times higher than that on CDs, with the largest enhancement occurring in NO₃⁻ (5.4 times), comparable increases in NH₄⁺, K⁺, Cl⁻ (approximately 4 times), and the smallest increase in OM (2.6 times), indicating that both primary emissions and secondary transformations contributed to the EG. A total of 3 EG episodes were analyzed in this study; 2 occurred in winter and 1 occurred in autumn, with a total duration of 21 h. The PM_{2.5} concentration in Ep3 was highest (135.7 $\mu\text{g m}^{-3}$), followed by that of Ep2 (129.6 $\mu\text{g m}^{-3}$), and that of Ep1 (82.3 $\mu\text{g m}^{-3}$). The contributions of chemical components were relatively similar in Ep2 and Ep3, and the highest contribution was NO₃⁻, while OM contributed the most in Ep1. The contribution of primary pollutants to Ep1 was greater than that to other EG events, while Ep2 and Ep3 were mainly affected by secondary aerosols. The high O₃ levels and stronger photochemical effects during Ep1 and Ep3 indicated that they were dominated by gas-phase oxidation reactions. The higher RH and contribution of secondary aerosols in Ep2 and Ep3 suggested that Ep2 and Ep3 were mainly influenced by heterogeneous reactions. This study indicated that stagnant weather conditions and chemical reaction processes made important contributions to the EG and improved our understanding of the causes of EG.

The contribution of SNA during EG (61%) was greater than that on CDs (53.1%); however, the contribution of OM exhibited the opposite distribution. In addition, among SNA, NO₃⁻ contributed the most during EG, rising from 21.1% on CDs to 31.1% during EG. Thus, we recommend paying more attention to secondary inorganic compounds in Shanghai, especially NO₃⁻.

Author Contributions: Conceptualization, W.S.; methodology, W.S.; investigation, J.H. and Q.F.; resources, J.H. and Q.F.; data curation, W.S.; writing—original draft preparation, W.S.; writing—review and editing, W.S., Y.Z. and X.L.; visualization, W.S.; supervision, W.S. and X.L.; project administration, W.S.; funding acquisition, W.S. All authors have read and agreed to the published version of the manuscript.

Funding: This research was funded by Shanghai Sailing Program, grant number 21YF1418400; Climbing Program by Shanghai University of Medicine and Health Sciences, grant number A3-0200-22-311008-2; the Scientific Research Fund of Shanghai University of Medicine and Health Sciences, grant number SSF-21-05-013; and the High-Level Local University Construction Program of Shanghai, grant number E1-2602-21-201006-1.

Institutional Review Board Statement: Not applicable.

Informed Consent Statement: Not applicable.

Data Availability Statement: Not applicable.

Conflicts of Interest: The authors declare no conflict of interest. The funders had no role in the design of the study; in the collection, analyses, or interpretation of data; in the writing of the manuscript; or in the decision to publish the results.

References

1. Zhong, J.; Zhang, X.; Dong, Y.; Wang, Y.; Liu, C.; Wang, J.; Zhang, Y.; Che, H. Feedback effects of boundary-layer meteorological factors on cumulative explosive growth of PM_{2.5} during winter heavy pollution episodes in Beijing from 2013 to 2016. *Atmos. Chem. Phys.* **2018**, *18*, 247–258. [\[CrossRef\]](#)
2. Li, Y.E.; Zhu, B.; Lei, Y.; Li, C.; Wang, H.; Huang, C.; Zhou, M.; Miao, Q.; Wei, H.; Wu, Y.; et al. Characteristics, formation, and sources of PM_{2.5} in 2020 in Suzhou, Yangtze River Delta, China. *Environ. Res.* **2022**, *212*, 113545. [\[CrossRef\]](#) [\[PubMed\]](#)
3. Amaladhasan, D.A.; Heyn, C.; Hoyle, C.R.; El Haddad, I.; Elser, M.; Pieber, S.M.; Slowik, J.G.; Amorim, A.; Duplissy, J.; Ehrhart, S.; et al. Modelling the gas-particle partitioning and water uptake of isoprene-derived secondary organic aerosol at high and low relative humidity. *Atmos. Chem. Phys.* **2022**, *22*, 244. [\[CrossRef\]](#)
4. He, K.; Yang, F.; Ma, Y.; Zhang, Q.; Yao, X.; Chan, C.K.; Cadle, S.; Chan, T.; Mulawa, P. The characteristics of PM_{2.5} in Beijing, China. *Atmos. Environ.* **2001**, *35*, 4959–4970. [\[CrossRef\]](#)
5. Chen, Z.; Xie, X.; Cai, J.; Chen, D.; Gao, B.; He, B.; Cheng, N.; Xu, B. Understanding meteorological influences on PM_{2.5} concentrations across China: A temporal and spatial perspective. *Atmos. Chem. Phys.* **2018**, *18*, 5343–5358. [\[CrossRef\]](#)
6. Zhang, X.; Zhong, J.; Wang, J.; Wang, Y.; Liu, Y. The interdecadal worsening of weather conditions affecting aerosol pollution in the Beijing area in relation to climate warming. *Atmos. Chem. Phys.* **2018**, *18*, 5991–5999. [\[CrossRef\]](#)
7. Li, R.; Cui, L.; Liang, J.; Zhao, Y.; Zhang, Z.; Fu, H. Estimating historical SO₂ level across the whole China during 1973–2014 using random forest model. *Chemosphere* **2020**, *247*, 125839. [\[CrossRef\]](#)
8. Ye, W.; Ma, Z.; Ha, X. Spatial-temporal patterns of PM_{2.5} concentrations for 338 Chinese cities. *Sci. Total Environ.* **2018**, *631*, 524–533. [\[CrossRef\]](#)
9. Zhai, B.; Chen, J. Development of a stacked ensemble model for forecasting and analyzing daily average PM_{2.5} concentrations in Beijing, China. *Sci. Total Environ.* **2018**, *635*, 644–658. [\[CrossRef\]](#)
10. Cheng, J.; Su, J.; Cui, T.; Li, X.; Dong, X.; Sun, F.; Yang, Y.; Tong, D.; Zheng, Y.; Li, Y.; et al. Dominant role of emission reduction in PM_{2.5} air quality improvement in Beijing during 2013–2017: A model-based decomposition analysis. *Atmos. Chem. Phys.* **2019**, *19*, 6125–6146. [\[CrossRef\]](#)
11. Wang, J.; Ge, X.; Sonya, C.; Ye, J.; Lei, Y.; Chen, M.; Zhang, Q. Influence of regional emission controls on the chemical composition, sources, and size distributions of submicron aerosols: Insights from the 2014 Nanjing Youth Olympic Games. *Sci. Total Environ.* **2022**, *807*, 150869. [\[CrossRef\]](#) [\[PubMed\]](#)
12. Sun, W.; Wang, D.; Yao, L.; Fu, H.; Fu, Q.; Wang, H.; Li, Q.; Wang, L.; Yang, X.; Xian, A.; et al. Chemistry-triggered events of PM_{2.5} explosive growth during late autumn and winter in Shanghai, China. *Environ. Pollut.* **2019**, *254*, 112864. [\[CrossRef\]](#) [\[PubMed\]](#)
13. Li, R.; Hu, Y.; Li, L.; Fu, H.; Chen, J. Real-time aerosol optical properties, morphology and mixing states under clear, haze and fog episodes in the summer of urban Beijing. *Atmos. Chem. Phys.* **2017**, *17*, 5093. [\[CrossRef\]](#)
14. Xuan, X.; Chen, Z.; Gong, Y.; Shen, H.; Shiyi, C. Partitioning of hydrogen peroxide in gas-liquid and gas-aerosol phases. *Atmos. Chem. Phys.* **2020**, *20*, 5513–5526. [\[CrossRef\]](#)
15. Leng, C.; Duan, J.; Xu, C.; Zhang, H.; Wang, Y.; Wang, Y.; Li, X.; Kong, L.; Tao, J.; Zhang, R.; et al. Insights into a historic severe haze event in Shanghai: Synoptic situation, boundary layer and pollutants. *Atmos. Chem. Phys.* **2016**, *16*, 9221–9234. [\[CrossRef\]](#)
16. Sun, W.; Huo, J.; Li, R.; Wang, D.; Yao, L.; Fu, Q.; Feng, J. Effects of energy structure differences on chemical compositions and respiratory health of PM_{2.5} during late autumn and winter in China. *Sci. Total Environ.* **2022**, *824*, 153850. [\[CrossRef\]](#)
17. Wang, Y.; Yao, L.; Wang, L.; Liu, Z.; Ji, D.; Tang, G.; Zhang, J.; Sun, Y.; Hu, B.; Xin, J. Mechanism for the formation of the January 2013 heavy haze pollution episode over central and eastern China. *Sci. China Earth Sci.* **2013**, *57*, 14–25. [\[CrossRef\]](#)
18. Zhang, R.; Jing, J.; Tao, J.; Hsu, S.C.; Wang, G.; Cao, J.; Lee, C.S.L.; Zhu, L.; Chen, Z.; Zhao, Y.; et al. Chemical characterization and source apportionment of PM_{2.5} in Beijing: Seasonal perspective. *Atmos. Chem. Phys.* **2013**, *13*, 7053–7074. [\[CrossRef\]](#)
19. Fang, X.; Fan, Q.; Liao, Z.; Xie, J.; Xu, X.; Fan, S. Spatial-temporal characteristics of the air quality in the Guangdong–Hong Kong–Macau Greater Bay Area of China during 2015–2017. *Atmos. Environ.* **2019**, *210*, 14–34. [\[CrossRef\]](#)
20. Zhou, S.; Yang, L.; Gao, R.; Wang, X.; Gao, X.; Nie, W.; Xu, P.; Zhang, Q.; Wang, W. A comparison study of carbonaceous aerosols in a typical North China Plain urban atmosphere: Seasonal variability, sources and implications to haze formation. *Atmos. Environ.* **2017**, *149*, 95–103. [\[CrossRef\]](#)
21. Tao, J.; Zhang, L.; Gao, J.; Wang, H.; Chai, F.; Wang, S. Aerosol chemical composition and light scattering during a winter season in Beijing. *Atmos. Environ.* **2015**, *110*, 36–44. [\[CrossRef\]](#)
22. Hao, J.M.; Wang, L.T.; Li, L.; Hu, J.N.; Yu, X.C. Air pollutants contribution and control strategies of energy-use related sources in Beijing. *Sci. China Ser. D* **2005**, *48*, 138–146.
23. Duan, F.K.; Liu, X.D.; He, K.B.; Lu, Y.Q.; Wang, L. Atmospheric aerosol concentration level and chemical characteristics of water-soluble ionic species in wintertime in Beijing, China. *J. Environ. Monit.* **2003**, *5*, 569–573. [\[CrossRef\]](#) [\[PubMed\]](#)
24. Zhang, X.Y.; Wang, Y.Q.; Zhang, X.C.; Guo, W.; Gong, S.L. Carbonaceous aerosol composition over various regions of China during 2006. *J. Geophys. Res. Atmos.* **2008**, *113*, D14111. [\[CrossRef\]](#)
25. Wang, H.; Tian, M.; Chen, Y.; Shi, G.; Liu, Y.; Yang, F.; Zhang, L.; Deng, L.; Yu, J.; Peng, C.; et al. Seasonal characteristics, formation mechanisms and source origins of PM_{2.5} in two megacities in Sichuan Basin, China. *Atmos. Chem. Phys.* **2018**, *18*, 865–881. [\[CrossRef\]](#)
26. Zhao, M.; Huang, Z.; Qiao, T.; Zhang, Y.; Xiu, G.; Yu, J. Chemical characterization, the transport pathways and potential sources of PM_{2.5} in Shanghai: Seasonal variations. *Atmos. Res.* **2015**, *158*, 66–78. [\[CrossRef\]](#)

27. Zheng, X.Y.; Liu, X.D.; Zhao, F.H.; Duan, F.K.; Yu, T.; Cachier, H. Seasonal characteristics of biomass burning contribution to Beijing aerosol. *Sci. China Ser. B* **2005**, *48*, 481–488. [[CrossRef](#)]
28. He, K.; Zhao, Q.; Ma, Y.; Duan, F.; Yang, F.; Shi, Z.; Chen, G. Spatial and seasonal variability of PM_{2.5} acidity at two Chinese megacities: Insights into the formation of secondary inorganic aerosols. *Atmos. Chem. Phys.* **2012**, *12*, 1377–1395. [[CrossRef](#)]
29. Wang, H.; Peng, Y.; Zhang, X.; Liu, H.; Zhang, M.; Che, H.; Cheng, Y.; Zheng, Y. Contributions to the explosive growth of PM_{2.5} mass due to aerosol–radiation feedback and decrease in turbulent diffusion during a red alert heavy haze in Beijing–Tianjin–Hebei, China. *Atmos. Chem. Phys.* **2018**, *18*, 17717–17733. [[CrossRef](#)]
30. Li, R.; Zhao, Y.; Zhou, W.; Meng, Y.; Zhang, Z.; Fu, H. Developing a novel hybrid model for the estimation of surface 8 h ozone (O₃) across the remote Tibetan Plateau during 2005–2018. *Atmos. Chem. Phys.* **2020**, *20*, 6175. [[CrossRef](#)]
31. Squizzato, S.; Masiol, M.; Brunelli, A.; Pistollato, S.; Tarabotti, E.; Rampazzo, G.; Pavoni, B. Factors determining the formation of secondary inorganic aerosol: A case study in the Po Valley (Italy). *Atmos. Chem. Phys.* **2013**, *13*, 1927–1939. [[CrossRef](#)]
32. Wang, D.; Zhou, B.; Fu, Q.; Zhao, Q.; Zhang, Q.; Chen, J.; Yang, X.; Duan, Y.; Li, J. Intense secondary aerosol formation due to strong atmospheric photochemical reactions in summer: Observations at a rural site in eastern Yangtze River Delta of China. *Sci. Total Environ.* **2016**, *571*, 1454–1466. [[CrossRef](#)] [[PubMed](#)]
33. Yassaa, N.; Meklati, B.Y.; Cecinato, A.; Marino, F. Organic aerosols in urban and waste landfill of Algiers metropolitan area: Occurrence and sources. *Environ. Sci. Technol.* **2001**, *35*, 306–311. [[CrossRef](#)] [[PubMed](#)]
34. Chow, J.C.; Watson, J.G.; Lu, Z.Q.; Lowenthal, D.H.; Frazier, C.A.; Solomon, P.A.; Thuillier, R.H.; Magliano, K. Descriptive analysis of PM_{2.5} and PM₁₀ at regionally representative locations during SJVAQS/AUSPEX. *Atmos. Environ.* **1996**, *30*, 2079–2112. [[CrossRef](#)]
35. Cesari, D.; Donato, A.; Conte, M.; Merico, E.; Giangreco, A.; Giangreco, F.; Contini, D. An inter-comparison of PM_{2.5} at urban and urban background sites: Chemical characterization and source apportionment. *Atmos. Res.* **2016**, *174*, 106–119. [[CrossRef](#)]
36. Strader, R.; Lurmann, F.; Pandis, S.N. Evaluation of secondary organic aerosol formation in winter. *Atmos. Environ.* **1999**, *33*, 4849–4863. [[CrossRef](#)]
37. Zhang, Y.; Huang, W.; Cai, T.; Fang, D.; Wang, Y.; Song, J.; Hu, M.; Zhang, Y. Concentrations and chemical compositions of fine particles (PM_{2.5}) during haze and non-haze days in Beijing. *Atmos. Res.* **2016**, *174*, 62–69. [[CrossRef](#)]
38. Zheng, G.J.; Duan, F.K.; Su, H.; Ma, Y.L.; Cheng, Y.; Zheng, B.; Zhang, Q.; Huang, T.; Kimoto, T.; Chang, D.; et al. Exploring the severe winter haze in Beijing: The impact of synoptic weather, regional transport and heterogeneous reactions. *Atmos. Chem. Phys.* **2015**, *15*, 2969–2983. [[CrossRef](#)]
39. Zhao, X.J.; Zhao, P.S.; Xu, J.; Meng, W.; Pu, W.W.; Dong, F.; He, D.; Shi, Q.F. Analysis of a winter regional haze event and its formation mechanism in the North China Plain. *Atmos. Chem. Phys.* **2013**, *13*, 5685–5696. [[CrossRef](#)]
40. Hua, W.; Chen, Z.M.; Jie, C.Y.; Kondo, Y.; Hofzumahaus, A.; Takegawa, N.; Chang, C.C.; Lu, K.D.; Miyazaki, Y.; Kita, K.; et al. Atmospheric hydrogen peroxide and organic hydroperoxides during PRIDE-PRD'06, China: Their concentration, formation mechanism and contribution to secondary aerosols. *Atmos. Chem. Phys.* **2008**, *8*, 6755–6773. [[CrossRef](#)]
41. Tian, M.; Wang, H.; Chen, Y.; Yang, F.; Zhang, X.; Zou, Q.; Zhang, R.; Ma, Y.; He, K. Characteristics of aerosol pollution during heavy haze events in Suzhou, China. *Atmos. Chem. Phys.* **2016**, *16*, 7357–7371. [[CrossRef](#)]
42. Tian, M.; Wang, H.; Chen, Y.; Zhang, L.; Shi, G.; Liu, Y.; Yu, J.; Zhai, C.; Wang, J.; Yang, F. Highly time-resolved characterization of water-soluble inorganic ions in PM_{2.5} in a humid and acidic mega city in Sichuan Basin, China. *Sci. Total Environ.* **2017**, *580*, 224–234. [[CrossRef](#)] [[PubMed](#)]
43. Chen, D.; Cui, H.; Zhao, Y.; Yin, L.; Lu, Y.; Wang, Q. A two-year study of carbonaceous aerosols in ambient PM_{2.5} at a regional background site for western Yangtze River Delta, China. *Atmos. Res.* **2017**, *183*, 351–361. [[CrossRef](#)]